Comparative Morphological Study of Poly(dioxolane)/Poly(methyl methacrylate) Segmented Networks and Blends by ^{13}C Solid-State NMR and Thermal Analysis

P. Adriaensens, L. Storme, R. Carleer, and J. Gelan*

Limburg University, Institute for Materials Research (IMO), Department SBG, Universitaire Campus, Building D, B-3590 Diepenbeek, Belgium

F. E. Du Prez*

Polymer Chemistry Division, Department of Organic Chemistry, Ghent University, Krijgslaan 281 S4bis, B-9000 Gent, Belgium

Received October 12, 2001

ABSTRACT: Nanostructured amphiphilic segmented networks based on poly(1,3-dioxolane) (PDXL) and poly(methyl methacrylate) (PMMA) have been synthesized by radical copolymerization of α,ω-diacrylate PDXL with methyl methacrylate (MMA). The corresponding polymer blends have been prepared by the radical polymerization of MMA in the presence of α,ω-dihydroxy-PDXL. The multiphase behavior of the segmented networks and polymer blends have been compared by making use of solid-state ^{13}C CP/MAS NMR spectroscopy, dynamic mechanical analysis (DMA), differential scanning calorimetry (DSC), and thermogravimetrical analysis (TGA). For the network structures, the combined analysis of the proton spin−lattice relaxation times (T_{1H}) and proton spin-lock relaxation times ($T_{1\rho H}$) revealed small PDXL domain sizes between 1 and 20 nm. DSC and DMA analysis also showed the forced compatibility of the network components. In the case of the polymer blends, the phase morphology strongly depends on the PDXL weight fraction. For blends with PDXL fractions higher than 20 wt %, T_{1H} relaxometry, DSC, and DMA analysis evidenced the presence of a heterogeneous phase morphology (domain sizes > 20 nm) that allows for the crystallization of the PDXL-rich domains.

Introduction

Segmented polymer networks (SPNs) belong to the category of cross-linked multicomponent polymer materials. Such materials are generated by grafting of polymer A to polymer B at both chain ends.[1] For that reason, intrinsically immiscible polymers could be combined by permanent fixations. In this way, SPNs differ from the extensively studied interpenetrating polymer networks (IPNs), in which two (or more) polymers are combined in network form without mutual connections between them. Several preparation methods for the formation of well-defined SPNs with good control of molecular weight between the cross-links and of the number of branches at the junction points have been described in the literature.[2−6] Most of them make use of telechelics or bis-macromonomers as their preparation precedes the network formation. Recently, the potential technological importance of this class of network architectures have been demonstrated for a wide range of applications such as biomaterials,[7] membranes,[8] solid-phase extraction,[9] templates for nanosized assemblies,[10] etc. This multipurpose character originates from their controllable nanostructure, which is the result of a unique phase morphology development during the simultaneous cross-linking and phase separation process. Although the first systematic morphological study on an interesting subclass of the SPNs, the so-called amphiphilic polymer conetworks, have been performed by microscopy techniques and small-angle X-ray scattering,[10] more effort is necessary to correlate the nanometer scale domain structures with their physical properties. In this paper, the authors want to contribute to this research by making use of solid-state high-resolution ^{13}C NMR and dynamic mechanical analysis (DMA) for the detailed characterization of SPNs on micro- and macroscale, respectively. The study has been focused on networks composed of hydrophilic, semicrystalline poly(1,3-dioxolane) (PDXL) and hydrophobic poly(methyl methacrylate) (PMMA). It has been shown in a previous study that such amphiphilic materials, in which the hydrophilic PDXL segments act as a polymeric cross-linker for the hydrophobic PMMA chains, can be applied as pervaporation membranes for the dehydration process of water/ethanol mixtures.[8]

In the present study, SPNs with varying PDXL/PMMA ratio and the corresponding polymer blends have been prepared. Their phase morphology will be evaluated and compared by T_{1H} and $T_{1\rho H}$ relaxation time studies and DMA analysis.

Experimental Section

Starting Materials. Toluene (Aldrich, HPLC grade) has been dried before use by refluxing over sodium wire. Dichloromethane was distilled twice over CaH_2, followed by drying under reflux on sodium−lead alloy for several hours. It was stored in the dark in the presence of sodium wires. Methyl trifluoromethanesulfonate (methyl triflate, Aldrich) was purified by distillation over CaH_2 just before use. Trifluoromethanesulfonic acid (triflic acid, Aldrich) was vacuum-distilled ((bp 46 °C/15 mmHg). 1,3-Dioxolane (DXL, Aldrich, 99%) was purified by distillation (three times) over CaH_2 and dried on sodium wire under reflux. Methyl methacrylate (MMA) was purified by distillation in the presence of a radical inhibitor, phenothiazine. Benzoyl peroxide (BPO, 97%) was used as received.

* Corresponding authors. J. Gelan: phone (32)11/268312, Fax (32)11/268301, e-mail jan.gelan@luc.ac.be. F. Du Prez: phone (32)9/2644503, Fax (32)9/2644972, e-mail filip.duprez@rug.ac.be.

10.1021/ma0117763 CCC: $22.00
Published on Web 04/11/2002

Preparation of α,ω-Diacrylate-PDXL and α,ω-Dihydroxy-PDXL. The experimental procedure for the synthesis of α,ω-diacrylate-PDXL has been described in detail.[11,12] Briefly, the cationic ring-opening polymerization of DXL occurs in dichloromethane with methyl trifluoromethanesulfonate as initiator and methylene−bis(oxyethyl acrylate) as transfer reagent. This transfer agent was obtained by the reaction of hydroxyethyl acrylate with paraformaldehyde under acid catalysis.[11] After stirring the reaction mixture at room temperature for 3 h, triethylamine is added to the mixture, and the α,ω-diacrylate PDXL is precipitated in cold ether and dried under vacuum. A similar procedure, described by Franta and Reibel,[13,14] has been applied for the synthesis of α,ω-dihydroxy-PDXL. For this synthesis, 1,4-butanediol is used in combination with trifluoromethanesulfonic acid as initiator system.

For this work, α,ω-diacrylate- and α,ω-dihydroxy-PDXL with a number-average molecular weight of about 4000 and an acrylate or hydroxyl functionality close to two have been prepared (characterized by GPC and NMR).

Segmented Networks and Polymer Blends. Certain amounts of MMA and of α,ω-diacrylate-PDXL, according to the desired weight ratio, are mixed vigorously with 1 wt % BPO (relative to vinyl monomer) at 50 °C for 3 min. For the synthesis of the networks with a high content of PDXL (60 wt %), a minimal amount of toluene is added to obtain a homogeneous and less viscous reaction mixture. The viscous solution was degassed for a few seconds before transferring it, by means of a syringe, between two glass plates that are kept at the desired distance (ultimate film thickness) by a silicone rubber spacer. Before use, the glass plates were treated with H_2SO_4 (95%) and with a solution (10%) of trimethylsilyl chloride in toluene to facilitate the recovery of the film after preparation. The glass plate mold containing the solution was kept in an oven for 80 min at 60 °C, 3 h at 80 °C, and 12 h at 110 °C. All films were subjected to a heat treatment for 12 h in a vacuum oven at 100 °C. A piece of each film was treated in a Soxhlet apparatus with boiling ethanol for 12 h. Only films with an extractable fraction of less than 5 wt % have been retained for further characterization. The low extractable fractions indicate an almost complete copolymerization between MMA and the bis-macromonomer.

The PDXL/PMMA polymer blends have been prepared by the same procedure. Instead, α,ω-dihydroxy-PDXL (M_n = 3950 g/mol) has been mixed in the desired weight ratio with MMA and 1 wt % BPO.

Instruments. Solution-state ^{1}H NMR spectra of PDXL were recorded in $CDCl_3$ on a Bruker Advance 500-NMR apparatus. The molecular weights were determined by gel permeation chromatography using a 60 cm 10^3 Å column from Toyo Soda Manufacturing Co. and a Melz RI (LCD212) detector with chloroform as an eluent at a flow rate of 1.0 mL/min (polystyrene standards).

Values of E', E'', and tan δ were measured in the dual cantilever mode by a TA Instruments DMA 2980 apparatus on rectangular films of 1 mm thickness at a heating rate of 2 °C/min and at a frequency of 1 Hz. Thermogravimetrical analysis was performed with a Polymer Laboratories TGA, type PL-TG 1000 under N_2 atmosphere and heating rate of 10 °C/min.

DSC's were recorded on a Perkin-Elmer 7 with thermal analysis controller TAC 7/DX. After keeping the samples at 110 °C in the DSC apparatus, the temperature was decreased to −20 °C (crystallization temperature of PDXL) and held there for 15 min. Then, the samples were quenched (−90 °C) and finally heated at a rate of 10 °C/min.

Solid-state ^{13}C CP/MAS NMR spectra were recorded at ambient temperature on an Inova 400 Varian spectrometer operating at a static magnetic field of 9.4 T. Magic angle spinning was performed at 6.0 kHz, making use of ceramic Si_3N_4 rotors. The aromatic signal of hexamethylbenzene was used to determine the Hartmann−Hahn condition ($\omega_{1H} = \gamma_H\beta_{1H} = \gamma_C\beta_{1C} = \omega_{1C}$) for cross-polarization and to calibrate the carbon chemical shift scale (132.1 ppm). Other spectral parameters used were a 90° pulse length of 5.0 μs, a spectral width of 50 kHz, an acquisition time of 35 ms, a recycle delay of 4.2 s, and 1250 repetitions. High-power decoupling was set to 65 kHz during the acquisition time. The proton spin−lattice (T_{1H}) and spin−lattice relaxation time in the rotating frame ($T_{1\rho H}$) were measured via the carbon nuclei by means of a multipurpose pulse sequence[15] in which a fixed contact time of 800 μs was used for cross-polarization. The spin-lock field was set to 50 kHz. A pulse delay of 5 times the longest T_{1H} value has been used for the determination of the $T_{1\rho H}$ relaxation times. The $T_{1\rho H}$ values have been derived using eq 1:

$$M(t) = \sum M_0^{\,i} \exp(-(\mathrm{CT} + t)/\, T_{1\rho H}^{\,i}) \qquad (1)$$

In this equation, $M(t)$ is the overall magnetization as a function of the variable evolution time t and CT is the fixed cross-polarization contact time. $M_0^{\,i}$ and $T_{1\rho H}^{\,i}$ refer to the fraction (percent) and time constant, respectively, of the different phase-separated domains.

All nonlinear least-squares analyses of relaxation data have been performed on a Macintosh computer using the program Kaleidagraph 3.0.

Results and Discussion

A. Synthesis of Telechelic Poly(1,3-dioxolane) Chains. 1,3-Dioxolane (DXL) belongs to the class of heterocyclic monomers containing acetal functions that only polymerize cationically.[16] A specific characteristic of DXL is its lower nucleophilicity as compared to that of the acetal functions in PDXL. Thus, in competition with the propagation reaction, the active sites at the growing polymer ends, i.e., cyclic dioxolenium cations, will also be involved in a reaction with the acetal functions in the polymer chains.[17,18] This continuous transacetalization process results in a broadening of the molecular weight distribution and in the formation of cyclic structures.[19] It has been shown that these intermolecular transfer reactions can be applied to introduce reactive end groups on both chain ends of PDXL by the addition of a low molar mass formal as chain transfer agent during the polymerization. By the introduction of two acrylate end groups on this transfer agent, this synthetic process leads to α,ω-diacrylate-PDXL chains.[12,20] The molecular weight of the linear polymers is governed by the ratio of reacted monomer to transfer agent and is generally well controlled up to 10 000 g/mol.

The synthesis of α,ω-dihydroxy-PDXL chains is based on the activated monomer mechanism.[21] Franta et al. have established that when DXL is polymerized by strong protonic acids, such as triflic acid, in the presence of a diol, the PDXL chains are essentially linear and carry end-standing OH functions. Despite the occurrence of some side reactions, this mechanism leads to α,ω-dihydroxy-PDXL, the molecular weight of which is controlled by the molar ratio of DXL consumed to diol introduced.[13] It has been shown that the amount of cyclic species formed is negligible, that the dispersity is on the order of 1.4, and that molar masses up to 10 000 g/mol can be covered.

B. Synthesis of Segmented Networks and Polymer Blends. The general procedure for the synthesis of block copolymer networks, further referred to as segmented networks, consists of a free radical copolymerization of bis-macromonomers with vinyl monomers in the presence of a radical thermal initiator.[20,22] In this work, α,ω-diacrylate-PDXL (M_n = 4000) has been used as polymeric cross-linking agent for PMMA. Transparent, mechanically stable PDXL/PMMA segmented network films with three different weight fractions of PDXL, about 20%, 40%, and 60%, have been prepared for the solid-state NMR and thermal analysis studies.

More detailed information about the synthesis, soluble fractions, swelling behavior, and pervaporation properties can be found elsewhere.[8] The networks are coded as illustrated in the following example: *net*-poly(DXL-(40)-*co*-MMA(60)). In this network, 40% PDXL bismacromonomer has been copolymerized with 60% MMA. For convenience sake, a shorter abbreviation will be used such as "network 40/60", in which the first number always indicates the PDXL content.

For the preparation of the corresponding PDXL/PMMA polymer blends, MMA has been radically polymerized to linear PMMA in the presence of α,ω-dihydroxy-PDXL under the same reaction conditions as for the segmented networks. The hydroxyl end groups of this telechelic polymer allow for the in situ preparation of polymer blends, as they do not interfere with the PMMA formation. An abbreviation such as "blend 40/60" will be used, in accordance with that for the networks, to indicate the fractions of the two components in the blends. All the polymer blends have been prepared in the form of rectangular films. The blend 20/80 is a transparent material while blends with larger PDXL fractions are opaque, brittle materials.

C. Solid-State NMR and Thermal Analysis of Segmented Networks. For rigid polymer systems below the glass transition temperatures (T_g), the proton relaxation times T_{1H} and $T_{1\rho H}$ provide information about the level of heterogeneity (morphology) on the nanometer scale due to the process of proton spin diffusion.[23] Under the condition of efficient spin diffusion, the two proton relaxation times can be directly related to the sizes of molecular domains. The proton $T_{1\rho H}$ decay time, on the order of milliseconds, will be averaged out over a short distance (on the order of 1−2 nm), making it a rather local property. Since the $T_{1\rho H}$ relaxation time is sensitive to frequency motions of several tens of kilohertz, it reflects the motion of short segments in the polymer chain. The T_{1H} decay time, on the other hand, on the order of seconds, is sensitive to the density of Larmor frequency motions (several hundred megahertz) and is averaged out over a larger distance (in the order of tens of nanometers), making it a more large-scale molecular property, like T_g. The maximum path length L, over which proton−proton spin diffusion can occur, is approximately given by $L \approx (6DT_i)^{1/2}$ where D is the spin diffusion coefficient ($= 10^{-16}$ m^2/s for rigid solids) and T_i is the relaxation time T_{1H} or $T_{1\rho H}$.[24] If the intrinsic relaxation times of the molecular domains are sufficiently different, multiple relaxation times will only be observed if the domain sizes are larger than L. Two options can be used to understand the relation between the values of the relaxation times and the molecular chain mobility: (a) determination of the decay times as a function of temperature or (b) as a function of the strength of the spin-lock field ($T_{1\rho H}$) or B_0 field (T_{1H}). This allows to situate the relaxation times on a log T_i− log τ_C correlation diagram (in which τ_c is the correlation time of molecular motion). In such a diagram three distinct regions can be evaluated. The region with very short τ_C times, characteristic for mobile molecules, where all relaxation times are equal and decrease as a function of increasing τ_C. A second region is situated around the minima of T_{1H} and $T_{1\rho H}$, where the spectral density of the megahertz motions (T_{1H}) or kilohertz motions ($T_{1\rho H}$) is optimal. In the third region, characteristic for the rigid materials with long τ_C's, T_{1H} as well as $T_{1\rho H}$ increases again as a function of increasing τ_C.

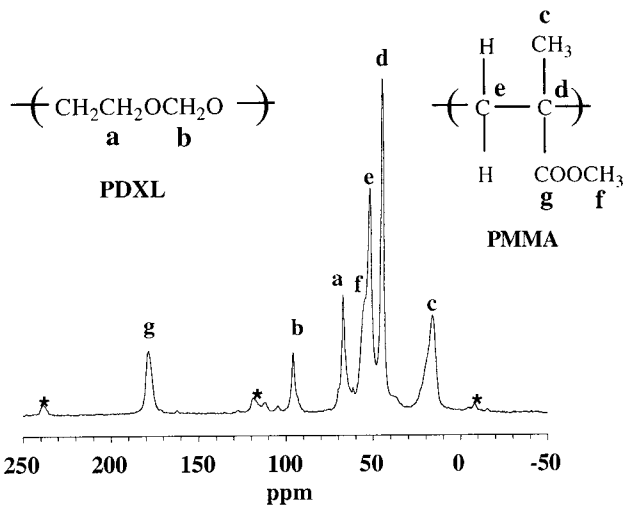

Figure 1. 100 MHz solid-state ^{13}C CP/MAS spectrum of a PDXL/PMMA segmented network. Peaks marked with an asterisk are spinning sidebands.

It is in this region that, for a given correlation time, T_{1H} increases with increasing the B_0 field strength and $T_{1\rho H}$ increases with increasing the strength of the spin-lock field.

Figure 1 shows a typical ^{13}C solid-state NMR spectrum of the network 60/40. The carbon resonances are assigned as depicted in Figure 1. Since the carbon resonances of PDXL are completely separated from those of PMMA, the investigation of the proton relaxation behavior of the two polymers can be investigated separately.

For the three polymer networks, a similar T_{1H} decay time of ca. 0.8 s was observed via all the carbon resonances of PMMA as well as via those of PDXL due to efficient spin diffusion of proton magnetization throughout the network (Table 1). This means that, if the networks have a phase-separated morphology, the domain sizes have to be smaller than about 20 nm.

Similar conclusions can be drawn from DMA analysis of the networks. The influence of the composition on the final morphology of the segmented networks, as expressed by the shape of their dissipation factor (tan δ) vs temperature curves, is illustrated in Figure 2.

For the investigated networks, separate transitions corresponding to the T_g's of the two components are not observed. For the networks 20/80 and 40/60 only a single averaged glass transition temperature is observed of 69 and 95 °C, respectively. This indicates the high degree of compatibility of the two polymer components in these networks. The temperature corresponding to this maximum is governed by the ratio of the two components and is generally higher than the one predicted by the equation of Fox for random copolymers.[25] This phenomenon is ascribed to the decrease of the polymer chain dynamics in the networks by the introduction of the junction points between them.[8] For the network with the highest PDXL content (curve 3 of Figure 2), a broadened transition with a clear inflection point, situated at higher temperature, is observed which demonstrates its microheterogeneous phase morphology. This observation already indicates that the thermodynamics of phase separation between PDXL and PMMA begin to rule the overall phase morphology and are not counterbalanced anymore by the forced compatibility between them.

Table 1. T_{1H} and $T_{1\rho H}$ Relaxation Times of the Segmented Networks[a]

networks	T_{1H} (s) PMMA	T_{1H} (s) PDXL	$T_{1\rho H}$ (ms) PMMA	$T_{1\rho H}^{L}$ (ms)/M_0^{L} (%) PDXL	$T_{1\rho H}^{S}$ (ms)/M_0^{S} (%) PDXL
20/80	0.81	0.81	9.4	9.3/47	1.0/53
40/60	0.79	0.78	7.1	6.8/32	0.9/68
60/40	0.79	0.79	5.5	5.3/34	1.0/66

[a] The averaged 95% confidence limit for T_{1H}, $T_{1\rho H}$, and M_0 is about 3%, 7%, and 10%, respectively. For $T_{1\rho H}$ of PDXL, the $T_{1\rho H}^{L}$ and $T_{1\rho H}^{S}$ fractions (M_0^{L} and M_0^{S}) are normalized to 100.

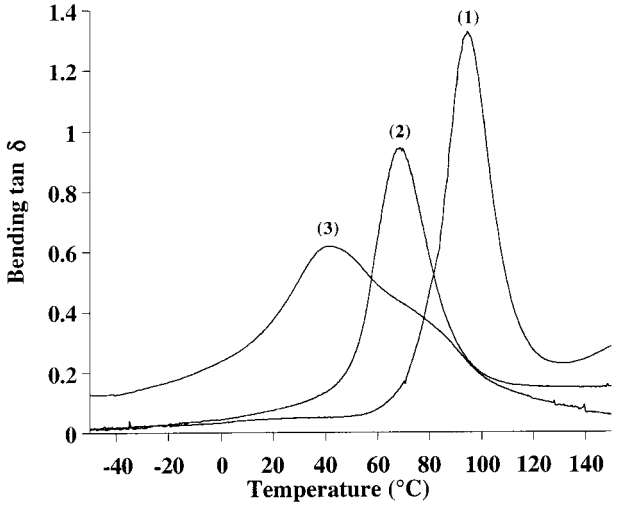

Figure 2. DMA curves of the different PDXL/PMMA segmented networks: (1) network 20/80; (2) network 40/60; (3) network 60/40.

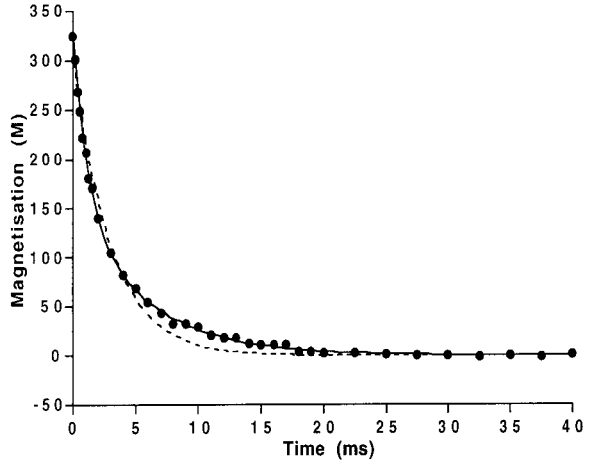

Figure 3. Example of a biexponential curve fit of the $T_{1\rho H}$ decay of PDXL in the PDXL/PMMA networks and the blends. The monoexponential fit is indicated by the dotted line.

Anyhow, the absence of separated T_g transitions, the absence of crystallization of PDXL-rich domains, as demonstrated by DSC and DMA analysis, and the results from the T_{1H} relaxation time analysis confirm that the networks are compatible on a scale of 20 nm.

For the investigation of the phase morphology on the nanometer scale, the $T_{1\rho H}$ decay times of the network components have been determined (Table 1). For the two PDXL carbon resonances, the $T_{1\rho H}$ decay behaves biexponentially, resulting in a short ($T_{1\rho H}^{S}$) and long ($T_{1\rho H}^{L}$) $T_{1\rho H}$ decay time (cf. eq 1), of which the fractions represent the amount of PDXL chains with different molecular chain mobility. The biexponential character of the $T_{1\rho H}$ decay of PDXL is clearly demonstrated in Figure 3, in which an example of a curve fit, in both mono- and biexponential mode, is given. Since the two decay times are closely similar for the OCH_2 and OCH_2-CH_2O carbon resonances, their averaged value is presented in Table 1.

The presence of two relaxation times is indicative for a heterogeneous PDXL chain dynamics on a length scale of 1−2 nm. This means that the dimension of the PDXL domains has to be situated between 1 and 20 nm. On the other hand, the $T_{1\rho H}$ decay time observed via all PMMA carbon resonances behaves monoexponentially and has a value which is similar to this of $T_{1\rho H}^{L}$ of PDXL (Table 1). Also, for PMMA only the averaged $T_{1\rho H}$ value observed via all five-carbon resonances is presented in Table 1.

With increasing PDXL fraction in the networks, an increase of the PMMA chain mobility is observed as expressed by the decreasing $T_{1\rho H}$ value of PMMA. Because of efficient spin diffusion between PMMA and the immobilized PDXL fraction, the $T_{1\rho H}^{L}$ of PDXL decreases in accordance with $T_{1\rho H}$ of PMMA. In the log T_i−log τ_C correlation diagram the $T_{1\rho H}$ decay times of PMMA and of immobilized PDXL are situated at the long correlation time side (slow molecular dynamics).[26] An increase of the PDXL fraction in the networks will therefore result in a decrease of τ_c (higher chain mobility) and a faster $T_{1\rho H}$ relaxation (smaller $T_{1\rho H}^{L}$ decay value). This is further confirmed by measurements, for all segmented networks, at a lower spin-lock field of 25 kHz which result in a decreased $T_{1\rho H}$ value of 3.5 ms for both PMMA and the immobilized PDXL fraction. ($T_{1\rho H}$ values are only dependent on the strength of the spin-lock field at the long τ_c side of the correlation diagram.)

From this it can be concluded that the long decay time $T_{1\rho H}^{L}$ represents amorphous PDXL chains that are constrained by the rigid PMMA chains due to the presence of chemical cross-links and physical entanglements. The short decay time $T_{1\rho H}^{S}$ of ca. 1 ms represents mobile amorphous PDXL chains, at longer distance from the rigid PMMA chains.

The varying level on which the PDXL and PMMA chains are mixed in the segmented networks is further expressed by the comparison of their degradation behavior (Figure 4).

From the TGA curves in Figure 4, it is observed that the degradation behavior strongly depends on the weight fraction of the constituting polymers. The linear homopolymer of PDXL degrades in the temperature interval between 150 and 220 °C in a N_2 atmosphere.[8] For the network 20/80, a rather continuous degradation of the network is observed in a temperature range of 150−400 °C. On the other hand, network 40/60 shows a two-step degradation; i.e., PDXL degrades in the region from 150 to 300 °C while PMMA degrades between 300 and 400 °C. For the network 60/40, the two-step degradation becomes even more obvious as the degradation corresponding to PDXL is completely shifted to lower temperatures, similar to the degradation behavior of linear PDXL. It seems that the degradation

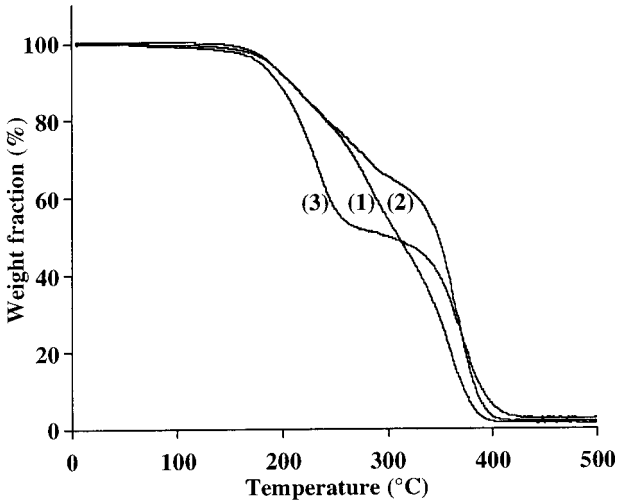

Figure 4. TGA curves of the different PDXL/PMMA segmented networks: (1) network 20/80; (2) network 40/60; (3) network 60/40.

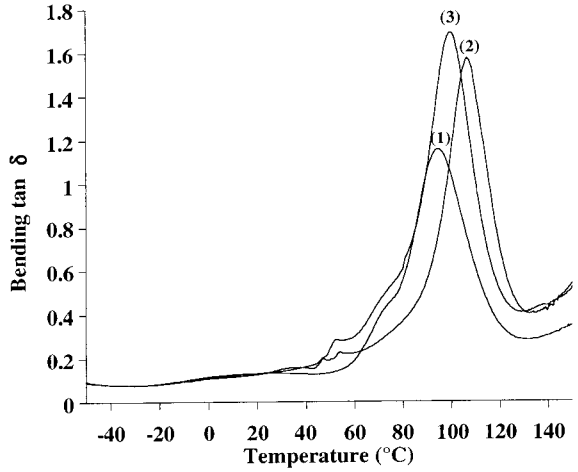

Figure 5. DMA curves of the different PDXL/PMMA blends: (1) blend 20/80; (2) blend 40/60; (3) blend 60/40.

of the PDXL chains in this latter network is much less influenced by that of the PMMA chains as compared to the other networks. It is suggested that the thermal stability of these mobile PDXL chains is comparable to that of linear PDXL because of the high amount of mobile PDXL. From Table 1, it can indeed be observed that the relative fraction of the mobile PDXL chains (M_0^S) increases from about 50 to 70% for increasing PDXL contents while $T_{1\rho H}^L$ decreases.

D. Solid-State NMR and Thermal Analysis of the Polymer Blends. In general, the polymer blends show a more heterogeneous phase morphology as compared to their network analogues. The DMA curves of the blends 40/60 and 60/40 show a major transition at about 100−110 °C, which differs significantly from the averaged glass transition temperature obtained for the corresponding networks (69 and 41 °C, respectively) (Figure 5). This clearly indicates phase separation for the PDXL-rich blends. It has been confirmed by DSC analysis that the small transitions at about 50 °C are to be ascribed to the melting process of crystalline PDXL domains. On the contrary, these crystalline domains are completely absent in the blend 20/80. The more extensive mixing of the two components in this blend, as compared to blends with higher PDXL fractions, is further demonstrated by DMA and by ^{13}C solid-state NMR relaxation studies. In the DMA analysis (curve 1), the major transition is situated at the same temperature (95 °C) as for the network 20/80, which indicates an extensive mixing of PMMA with the PDXL segments. The averaged glass transition temperature valorizes the conditions for spin diffusion for this blend 20/80.

Table 2 presents the T_{1H} and $T_{1\rho H}$ relaxation times for the corresponding blends. A similar T_{1H} decay time for all ^{13}C resonances of the two polymers in the blend 20/80 confirms efficient spin diffusion (Table 2). This means that, if molecular domains are present, they have to be smaller than 20 nm. On the other hand, two $T_{1\rho H}$ decay times are observed. For PDXL, a $T_{1\rho H}^L$ decay time of ca. 8 ms is found which is similar to the value observed for all carbon resonances of PMMA. As for the networks, a second $T_{1\rho H}^S$ decay time of ca. 1 ms is present for the PDXL resonances. Again, $T_{1\rho H}^L$ represents the fraction of amorphous PDXL chains that are immobilized by the rigid PMMA (interphase). It means that small PDXL domains with an estimated size between 1 nm ($T_{1\rho H}$) and 20 nm (T_{1H}) are present in the PMMA continuous phase.

Since the PDXL chains in the blends are only constrained by physical entanglements, a reduced fraction of immobilized PDXL chains (M_0^L) is observed as compared to the corresponding network. The decrease of the $T_{1\rho H}^L$ decay time from 9.4 ms for the network to ca. 8 ms for the corresponding blend reflects that the PDXL chains are less immobilized in the blend as compared to the network. This phenomenon can be ascribed to the absence of the chemical cross-links.

For the blends 40/60 and 60/40, phase separation has been demonstrated by DMA analysis. The PDXL-rich phase has a T_g below ambient temperature which prevents efficient spin diffusion with the PMMA. This means that different PMMA and PDXL T_{1H} decay times not necessarily stand for phase separation. However, since the DMA analysis is indicative for phase separation, the different T_{1H} decay times are representing the large (>20 nm) phase-separated PMMA and PDXL domains. This is further confirmed by the appearance of crystallization in the PDXL domains (see later). Because of phase separation, the T_{1H} decay time of the constituting blend components becomes dependent on the spectral density of molecular motions $J(\omega)$ in the megahertz range and the average proton environment in the separated domains.[27] The presence of large molecular domains in these blends results in the deviation of the two $T_{1\rho H}$ decay times of PDXL (1.6 and 6.8 ms) from the one (9.0 ms) observed for PMMA. Therefore, the three $T_{1\rho H}$ decay times have to originate from other phases than those described for the networks and for the blend 20/80; i.e., $T_{1\rho H}^L$ and $T_{1\rho H}^S$ no longer correspond to the fractions of the mobile and immobilized chains of the PDXL amorphous domains, respectively. The presence of small crystalline PDXL domains in the PDXL phase, as already demonstrated by DSC, should also be reflected in the $T_{1\rho H}$ decay times of these blends. Indeed, the two PDXL decay times can be assigned in accordance with a previous study on linear PDXL and PDXL networks.[28] In this study, a $T_{1\rho H}$ decay time of 5.7 and 1.1 ms was observed for the amorphous and crystalline PDXL domains, respectively. Consequently, the $T_{1\rho H}^L$ (6.8 ms) and $T_{1\rho H}^S$ (1.6 ms) can be ascribed to the mobile, elastomeric and rigid crystalline PDXL domains, respectively. This assignment is further confirmed by the results obtained at a weaker

Table 2. T_{1H} and $T_{1\rho H}$ Relaxation Times of the Polymer Blends[a]

	T_{1H} (s)				
blends	PMMA	PDXL	$T_{1\rho H}$ (ms) PMMA	$T_{1\rho H}^{L}$ (ms)/ M_0^{L} (%) PDXL	$T_{1\rho H}^{S}$ (ms)/ M_0^{S} (%) PDXL
20/80	0.80	0.80	8.0	8.0/30	0.9/70
40/60	0.80	1.10	9.0	6.8/65	1.6/35
60/40	0.91	1.10	9.0	6.8/70	1.6/30

[a] The averaged 95% confidence limit for T_{1H}, $T_{1\rho H}$, and M_0 is about 2%, 4%, and 7%, respectively. For $T_{1\rho H}$ of PDXL, the $T_{1\rho H}^{L}$ and $T_{1\rho H}^{S}$ fractions (M_0^{L} and M_0^{S}) are normalized to 100.

spin-lock field (25 kHz) which show that the molecular motions of the PDXL chains become independent of those of PMMA. At this spin-lock field, a similar $T_{1\rho H}^{L}$ value is observed meaning that this decay time is situated at the short τ_C side of the correlation diagram. ($T_{1\rho H}$ values are only dependent on the strength of the spin-lock field at the long τ_C side of the correlation diagram.) The PMMA $T_{1\rho H}$ decay time decreases from 9 to 4 ms upon decreasing the strength of the spin-lock field and is situated at the long τ_C side of the correlation diagram because of the reduced molecular mobility of the PMMA phase as compared to the phase-separated PDXL.

Conclusions

Solid-state ^{13}C CP/MAS NMR and thermal analysis were applied for the comparative investigation of the multiphase behavior of PDXL/PMMA segmented networks and blends. Analysis of the proton spin−lattice relaxation decay (T_{1H}) indicates a homogeneous phase morphology on a scale of 20 nm for the segmented networks. On the other hand, a heterogeneous phase morphology has been detected on a scale of 1−2 nm by means of proton spin-lock relaxation time measurements ($T_{1\rho H}$). For PDXL two decay times are observed; the short $T_{1\rho H}^{S}$ decay time is assigned to amorphous PDXL chains while the long $T_{1\rho H}^{L}$ decay time, being similar to the one observed for the PMMA resonances due to efficient spin diffusion, can be assigned to the amorphous PDXL chains that are constrained by chemical cross-links and entanglements with rigid PMMA chains. The forced compatibility of the network components on a scale of 20 nm, which prevents the crystallization of PDXL chains, is confirmed by DSC and DMA analysis. The decrease in compatibility of the two network components with increasing weight fraction of PDXL is reflected by a more obvious two-step degradation in the TGA curves.

For the blend 20/80, a similar compatibility behavior is observed as for the networks: homogeneously mixed on a more macroscopic scale (T_{1H}) but phase-separated on the nanometer level ($T_{1\rho H}$). An increase of the PDXL weight fraction in the blends results in phase-separated molecular domains having a dimension of at least 20 nm. In these blends (40/60 and 60/40) the phase-separated PDXL is able to crystallize as is demonstrated by DSC analysis and $T_{1\rho H}$ relaxometry.

This detailed comparative phase behavior study clearly demonstrated the forced compatibility of the two components in this unique type of segmented network architecture. The presence of their nanostructured morphology, which is the key to high-tech applications, has been confirmed.

Acknowledgment. The Belgian Programme on Interuniversity Attraction Poles initiated by the Belgian State, Prime Minister's Office, and the ESF Programme SUPERNET are acknowledged for financial support.

References and Notes

(1) Bamford, C. H.; Eastmond, G. C.; Whittle, D. *Polymer* **1969**, *10*, 771, 885.
(2) Liu, J.; Liu, W.; Zhou, H.; Hou, C.; Ni, S. *Polymer* **1991**, *32*, 1361.
(3) Chang, P. S.; Buese, M. A. *J. Am. Chem. Soc.* **1993**, *115*, 11475.
(4) Meier, W. *Macromolecules* **1998**, *31*, 2212.
(5) Ivan, B.; Kennedy, J. P.; Mackey, P. W. In *Polymer Drugs and Delivery Systems*; Dunn, R. L., Ottenbrite, R. M., Eds.; ACS Symp. Book Series 469; American Chemical Society: Washington, DC, 1991; pp 194−212.
(6) Du Prez, F. E.; Goethals, E. J. In *Ionic Polymerizations and Related Processes*; Puskas, J. E., Ed.; NATO Sci. Ser. E; Kluwer Academic Publishers: Dordrecht, The Netherlands, 1999; Vol. 359, pp 75−98.
(7) Kennedy, J. P.; Fenyvesi, G.; Na, S.; Keszler, B.; Rosenthal, K. S. *Des. Monomers Polym.* **2000**, *3*, 113.
(8) Du Prez, F. E.; Goethals, E. J.; Schué, R.; Qariouh, H.; Schué, F. *Polym. Int.* **1998**, *46*, 117.
(9) Reyntjens, W.; Jonckheere, L.; Goethals, E.; Du Prez, F. *Makromol. Chem., Macromol. Symp.* **2001**, *164*, 293.
(10) Scherble, J.; Thomann, R.; Ivan, B.; Mulhaupt, R. *J. Polym. Sci., Part B: Polym. Phys.* **2001**, *39*, 1429.
(11) Goethals, E. J.; De Clercq, R. R.; De Clercq, H. C.; Hartmann, P. J. *Makromol. Chem., Macromol. Symp.* **1991**, *47*, 151.
(12) De Clercq, R. R.; Goethals, E. J. *Macromolecules* **1992**, *25*, 1109.
(13) Franta, E.; Kubisa, P.; Refai, J.; Ould Kada, S.; Reibel, L. *Makromol. Chem., Macromol. Symp.* **1988**, *13/14*, 127.
(14) Franta, E.; Gérard, E.; Gnanou, Y.; Reibel, L.; Rempp, P. *Makromol. Chem.* **1990**, *191*, 1689.
(15) Hoogmartens, I.; Adriaensens, P.; Vanderzande, D.; Gelan, J. J. *Anal. Chim. Acta* **1993**, *283*, 1025.
(16) Plesch, P. H.; Westermann, P. H. *Polymer* **1969**, *10*, 105.
(17) Penczek, S.; Kubisa, P.; Matyaszewski, K. *Cationic Ringopening Polymerization of Heterocyclic Monomers*; *Adv. Polym. Sci.* 37; Springer-Verlag: Berlin, 1980.
(18) Ivin, K. J.; Saegusa, T. *Ringopening Polymerization*; Elsevier Publishers: Amsterdam, 1984; Vol. 1.
(19) Matyaszewski, K.; Zielinski, M.; Kubisa, P.; Slomokowski, S.; Chojnowski, J.; Penczek, S. *Makromol. Chem.* **1980**, *181*, 1469.
(20) Du Prez, F.; Goethals, E. J. *Macromol. Chem. Phys.* **1995**, *196*, 903.
(21) Penczek, S. *Polym. Prepr.* **1988**, *29*, 38.
(22) Ivan, B.; Kennedy, J. P.; Mackey, P. W. In *Polymer Drugs and Delivery Systems;* Dunn, R. L., Ottenbrite, R. M., Eds.; ACS Symposium Book Series 469; American Chemical Society: Washington, DC, 1991; p 194.
(23) Fedotov, V. D.; Schneider, H. *Structure and Dynamics of Bulk Polymers by NMR-Methods*; Springer-Verlag: Berlin, 1989.
(24) Douglas, D. C.; Jones, G. P. *J. Chem. Phys.* **1966**, *45*, 956.
(25) Fox, T. G. *Bull. Am. Phys. Soc.* **1956**, *1*, 123.
(26) Harris, R. K. *Nuclear Magnetic Resonance Spectroscopy, A Physochemical View;* Pitman Publishing Inc.: London, 1983.
(27) Sanders, J. K. M.; Hunter, B. K. *Modern NMR Spectroscopy;* Oxford University Press: New York, 1987.
(28) Du Prez, F. E.; Goethals, E. J.; Adriaensens, P. J.; Gelan, J. M.; Vanderzande, D. J. M. *Macromolecules* **1996**, *29*, 4000.

MA0117763